THE JOURNAL OF COMPARATIVE NEUROLOGY 401:129–143 (1998)

Distribution, Morphology, and γ-Aminobutyric Acid Immunoreactivity of Horizontally Projecting Neurons in the Macaque Inferior Temporal Cortex

HISASHI TANIGAWA,[1] ICHIRO FUJITA,[1,2,3]* MAKOTO KATO,[3] AND HISAYUKI OJIMA[4]

[1]Department of Cognitive Neuroscience, Osaka University Medical School, Osaka 565-0871, Japan
[2]Graduate School of Engineering Science, Osaka University, Osaka 565-8537, Japan
[3]Core Research for Evolutionary Science and Technology (CREST), Japan Science and Technology Corporation, Osaka 565-0871, Japan
[4]Department of Anatomy, Faculty of Medicine, Toho University, Omori-nishi, Ota, Tokyo 143-0015, Japan

ABSTRACT

In area TE of the macaque inferior temporal cortex, horizontal axons running parallel to the pial surface mediate interactions between laterally displaced sites across the cortex. We examined the spatial distribution and the types of cells that give rise to these horizontal axons, which are important factors in determining the nature of the lateral interactions in TE.

Intracortical injections of retrograde tracers labeled columnar clusters of cells and cells diffusely scattered within TE. The clusters were 0.35 ± 0.11 mm (mean ± SD) in diameter and were laterally distributed up to 6 mm from the injection site. Labeled cells were found in layers 2 to 6, with only a few labeled cells seen in layer 4. The clustering of labeled cells in layers 5 and 6 was looser than that in layers 2 and 3. Intracellular staining of the retrogradely labeled cells revealed that the majority of them were typical or modified pyramidal cells, both within and between the clusters. Only a few nonpyramidal interneurons were also stained at the fringe of the tracer injection site. Consistent with these results, only a small proportion of the retrogradely labeled cells exhibited γ-aminobutyric acid (GABA)-like immunoreactivity, mostly found within 1 mm from the injection site.

The results indicate that direct horizontal interactions in TE are predominantly mediated by pyramidal or modified pyramidal cells in layers 2, 3, 5, and 6 and are primarily excitatory in nature. The contribution of GABAergic interneurons to direct horizontal interactions is restricted to only short-distance projections. J. Comp. Neurol. 401:129–143, 1998.

Indexing terms: column; confocal imaging; GABA immunocytochemistry; horizontal axons; Lucifer Yellow; fluorescent latex beads

Cytoarchitectonic area TE, described by von Bonin and Bailey (1947), is the gyral part of the inferior temporal cortex in the macaque monkey and represents a higher association area in the cortical pathway crucial for object vision (Mishkin et al., 1983). Behavioral and physiological studies have revealed that TE plays an essential role in object discrimination and recognition (Gross, 1973; Dean, 1976; Logothetis and Sheinberg, 1996; Tanaka, 1996). In accordance with these complex tasks, neuroanatomical data on the afferent and efferent connections of TE indicate that it lies near the top of the hierarchy of the visual cortical areas and sends a major projection to the perirhinal cortex, which in turn innervates the entorhinal cortex and the hippocampus (Felleman and Van Essen, 1991; Suzuki, 1996). The intrinsic neuronal circuits within TE

Grant sponsor: CREST of the Japan Science and Technology Corporation; Grant sponsor: Uehara Memorial Foundation; Grant sponsor: Ministry of Education, Science, Sports and Culture; Grant numbers: 08279227 and 09268222.

*Correspondence to: Ichiro Fujita, Graduate School of Engineering Science, Osaka University, 1-3 Machikaneyama, Toyonaka, Osaka 560-8531, Japan. E-mail: ifujita@bpe.es.osaka-u.ac.jp

Received 26 February 1998; Revised 7 July 1998; Accepted 13 July 1998

have been largely unexplored in previous studies. At present, we have only limited insight into how this area is anatomically and functionally organized and how visual information is processed by the local circuits within TE.

One of the few known aspects of the functional architecture in TE that has been described is the columnar organization of neurons that respond to similar visual stimulus properties. These neurons are clustered radially to form columns across cortical layers (Fujita et al., 1992; Fujita, 1993; Tanaka, 1996). Neurons in adjacent columns respond to distinctly different features which, at least to researchers, do not appear to be related to each other (Fujita et al., 1992; but see Wang, G. et al., 1996, for face-selective columns). The columnar organization of TE may represent a discontinuous patchy map of visual sensory information on the cortical surface. This is in contrast to the primary visual cortex (V1; Hubel and Wiesel, 1977), which has a continuous map in which stimulus parameters are smoothly represented. Patchy brain maps may be advantageous in a system requiring both local and global levels of computation (Nelson and Bower, 1990), such as in TE where local computations may include sharpening of neuronal selectivity for specific object features, and global computations may involve the integration of the features represented in distant columns (Fujita, 1997).

TE, like V1 and other cortices, contains long-range horizontal axons running parallel to the cortical layers with intermittent patches of terminal arborizations appearing most prominently in layers 2 and 3 (Fujita and Fujita, 1996). These intrinsic horizontal axons connect distant sites in TE and are assumed to mediate communication between columns. Several morphological aspects of these horizontal axons reveal distinctions between the functional organization of V1 and TE: 1) In V1, the maximum extent of their projections is smaller (1.5–2 mm) than in TE (4–6 mm; Amir et al., 1993; Fujita and Fujita, 1996); 2) adjacent columnar sites in V1 have projection patches that largely overlap, whereas those in TE generally neither overlap nor abut each other (Tanigawa and Fujita, 1997); and 3) synaptic bouton density within the patches in V1 gradually decreases with increasing distance from the origin, a characteristic only weakly apparent in TE (H. Tanigawa, Q. Wang, and I. Fujita, unpublished observations).

In our efforts to further understand the nature of the interactions between the columns in TE compared to those in V1, we characterized in the present study the distribution and type of neurons in TE from which the horizontal axons originate. We analyzed the laminar and tangential distribution patterns of the horizontally projecting neurons using retrograde neuronal tracers, described their soma-dendritic morphology by injecting Lucifer Yellow intracellularly, and immunocytochemically identified whether they contain γ-aminobutyric acid (GABA). Preliminary results have appeared in abstract form (Fujita et al., 1995).

MATERIALS AND METHODS

Animals

Nine adult Japanese monkeys (*Macaca fuscata*) weighing 4.8–9.9 kg were used. Each animal received unilateral injections of one or two fluorescent retrograde tracers into the dorsal part of TE in order to label the cells of origin of the intrinsic horizontal axons (Fig. 1A; See Fujita and Fujita, 1996, for identification criteria of TE). The other hemispheres of these animals were used for other studies (Tanigawa and Fujita, 1997; Xu et al., 1997). The retrograde tracers used were Diamidino Yellow (DY, 2% in distilled water; Sigma, St. Louis, MO), Fast Blue (FB, 4% in distilled water; Dr. Illing, K.G. Makromolekulare Chemie, Grob-Umstadt, Germany), and green latex microspheres (fluorescein-labeled beads; hereafter referred to as "beads"; Lumafluor, Naples, FL; Katz and Iarovici, 1990). Seven monkeys received injections of DY. Five of these animals were used to examine the distribution pattern of retrogradely labeled cells, and the other two were used for

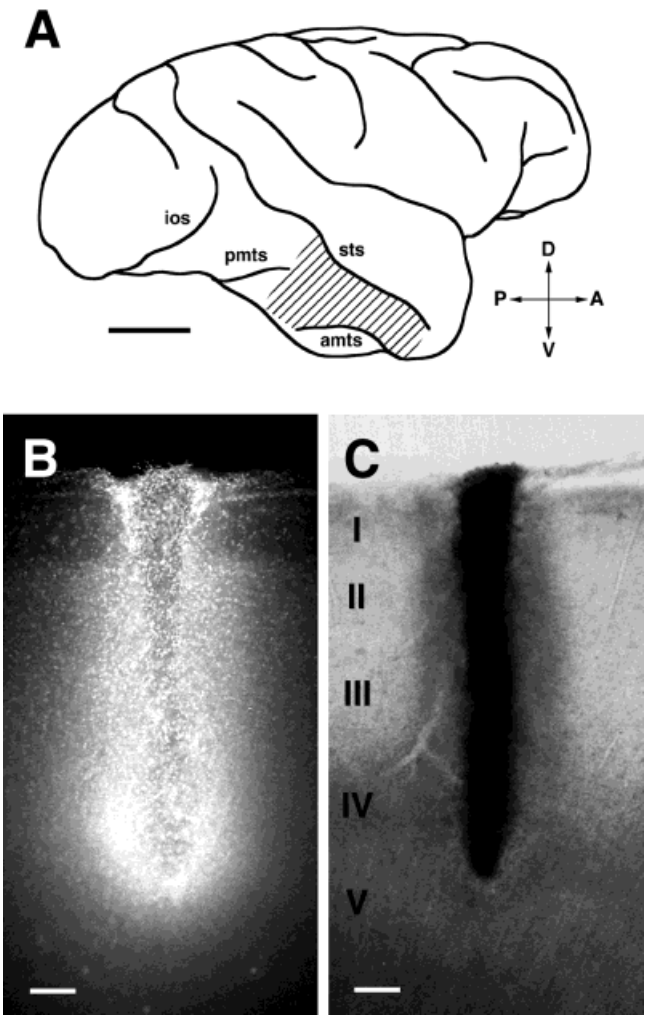

Fig. 1. **A:** Lateral view of a macaque right cerebral cortex. The hatched area indicates the dorsal part of area TE where we injected fluorescent tracers and examined retrograde labeling. amts, anterior middle temporal sulcus; ios, inferior occipital sulcus; pmts, posterior middle temporal sulcus; sts, superior temporal sulcus; A, anterior; P, posterior; D, dorsal; V, ventral. **B:** Fluorescent photomicrograph of a typical injection site (Diamidino Yellow, DY). **C:** Brightfield photomicrograph in the same region as in B. The injection core appears as a dark profile. The width of this injection core was 170 μm, smaller than that of a single TE column as previously shown (Fujita et al., 1992; Wang, G. et al., 1996; Fujita and Fujita, 1996). Scale bars = 10 mm in A, 200 μm in B,C.

morphological analysis of retrogradely labeled cells by intracellular injection of Lucifer Yellow CH (LY, 4% in distilled water; Sigma) into them. The remaining two monkeys, one injected with FB and the other with beads, were used for determining the possible GABA immunoreactivity of the retrogradely labeled cells.

Surgical procedures

Surgery was performed under aseptic conditions as described previously (Fujita and Fujita, 1996). All surgical and animal care procedures were in accordance with the guidelines of the Physiological Society of Japan (1988) and the National Institutes of Health (1996), and were approved by the animal experiment committee of Osaka University Medical School.

Prior to surgery, the animals were pretreated with atropine sulfate (0.02–0.03 mg/kg, i.m.) to reduce salivation and sedated with a mixture of ketamine hydrochloride (2.4–3.8 mg/kg, i.m.) and xylazine (1.0–1.5 mg/kg, i.m.). Animals were also given tranexaminic acid (10.1–22.2 mg/kg, i.m.) and carbazochrome sodium sulfate (0.5–1.1 mg/kg, i.m.) to minimize bleeding, and dexamethasone phosphate (0.1–0.2 mg/kg, i.m.) to prevent cortical edema. A catheter was inserted into the calf vein, and the animals were anesthetized with sodium pentobarbital (14–20 mg/kg, i.v.) and administered a glucose-saline solution (1 ml/kg/hr, i.v.). Additional doses of the anesthetics were administered as needed to maintain a surgical level of anesthesia. Body temperature was continuously monitored, and the animals were warmed with a heating pad to maintain the body temperature at around 37°C.

The scalp was incised, a large part of the temporal muscle was removed, and a craniotomy was performed to expose the dura over TE. Small incisions (0.5–1.0 mm) were made in the dura at the intended injection sites. After injections were completed according to the method described below, the dura was pulled over the incisions, the bone flap was replaced and cemented with dental acrylic resin, and the wound was sutured. The animals were administered an antibiotic, sodium piperacillin (22.4–44.4 mg/kg, i.m.), and an analgesic, ketoprofen (0.6–1.1 mg/kg, i.m.) on the day of surgery and daily for 1 week postoperatively. Treatment with dexamethasone was continued for 3 days after surgery with progressive withdrawal of the drug.

Retrograde labeling

Retrograde tracers were delivered through a glass micropipette (inner tip diameter 50–60 μm for FB and DY and 20–30 μm for beads) attached to the tip of a 1-μl Hamilton syringe. In seven cases, the tip of the pipette was first advanced to 2.0 mm below the pial surface and then withdrawn to the desired depth. To make cylindrical injection sites that extended throughout the thickness of the gray matter, a small volume of tracer (50–100 nl) was deposited at two depths, one aimed at the supragranular layer (0.7–1.0 mm) and the other aimed at the infragranular layer (1.6–1.8 mm). In the two other cases, in which we tried to confine DY injections to the supragranular layer, the tip was first lowered to 1.1–1.2 mm, and the tracer was deposited at a depth of 0.5–0.7 mm. The pipette was left in the cortex for 3–5 minutes after each tracer deposit. This procedure resulted in dye deposits of 170–510 μm in width covering either most of the layers or only the supragranular layers (Fig. 1B,C).

One to 3 weeks after the injections, the animals were deeply anesthetized with an overdose of sodium pentobarbital (60 mg/kg, i.v.). The monkeys received an intracardiac injection of heparin (1,000 I.U.), and the descending aorta was clamped. They were then perfused with fixatives. Fixation protocols differed depending on the experiment. Here we describe the protocol for the five monkeys that were exclusively investigated for retrograde labeling (see below for the protocols for LY injections and GABA immunocytochemistry). The five monkeys were perfused transcardially with 1 liter of 0.1 M phosphate-buffered saline (PBS; pH 7.4; 37°C) followed by 3–4 liters of 4% paraformaldehyde in chilled 0.1 M phosphate buffer (PB; pH 7.4) for 30–40 minutes. The animals were left for 90 minutes to allow the brain to harden, and then perfused with 2 liters of 10% and 1 liter of 20% sucrose in 0.1 M PB. The brains were removed from the skull, photographed, blocked, and stored in 30% buffered sucrose in 0.1 M PB until they sank. The surface of the blocks containing the injection sites was flattened by pressing it against aluminium foil-covered dry ice. The blocks were then cut tangentially to the surface into 50-μm-thick sections on a freezing microtome. The sections were mounted onto gelatin-coated slides, dried, rapidly dehydrated in absolute ethanol (5, 10, and 15 seconds), cleared in Hemo-De (5 and 15 seconds, Fischer Scientific, Chicago, IL), and coverslipped with Entellan (Merck, Darmstadt, Germany). The sections were stored in the dark at −20°C until the analysis was completed.

Lucifer Yellow injections

The two monkeys used for intracellular labeling were perfused with 1 liter of 0.9% NaCl (37°C) followed by 3 liters of 4% paraformaldehyde in 0.1 M PB. The brains were removed immediately, blocked, and postfixed in the same fixative for 90 minutes at 4°C. Blocks of tissue containing TE were cut with a Microslicer (DTK-3000; Dosaka, Kyoto, Japan) into alternate 200- and 300-μm-thick slices in a plane roughly perpendicular to the superior temporal sulcus (see Fig. 2A,B). Slices were rinsed and stored in cold 0.1 M PB.

Single 300-μm-thick slices were placed in a small chamber on the fixed stage of a microscope (Optiphot-2; Nikon, Tokyo, Japan) equipped with long-working distance objectives (SLWD series; Nikon), a B-2A filter block for observation of DY, and a V-2A filter block for observation of LY. Under visual guidance, DY-labeled neurons were impaled with glass micropipettes containing 4% LY by using a stage-mounted hydraulic micromanipulator (MW-4; Narishige, Tokyo, Japan; for details, see Ojima, 1993). The dye was injected iontophoretically by passage of a small current (2–10 nA negative current, 5–15 minutes). After injection into several neurons, the slices were rinsed in 0.1 M PB, postfixed in 4% paraformaldehyde in 0.1 M PB (1–2 hours), mounted onto slides, and coverslipped in 50% glycerin in 0.1 M PB. The remaining 200-μm-thick slices were used for examining the laminar distribution of retrogradely labeled neurons (Fig. 2C–G).

GABA immunocytochemistry

The two monkeys used for double labeling with a retrograde tracer and GABA immunocytochemistry were perfused with 200–300 ml of 160 mM sucrose, 0.1%

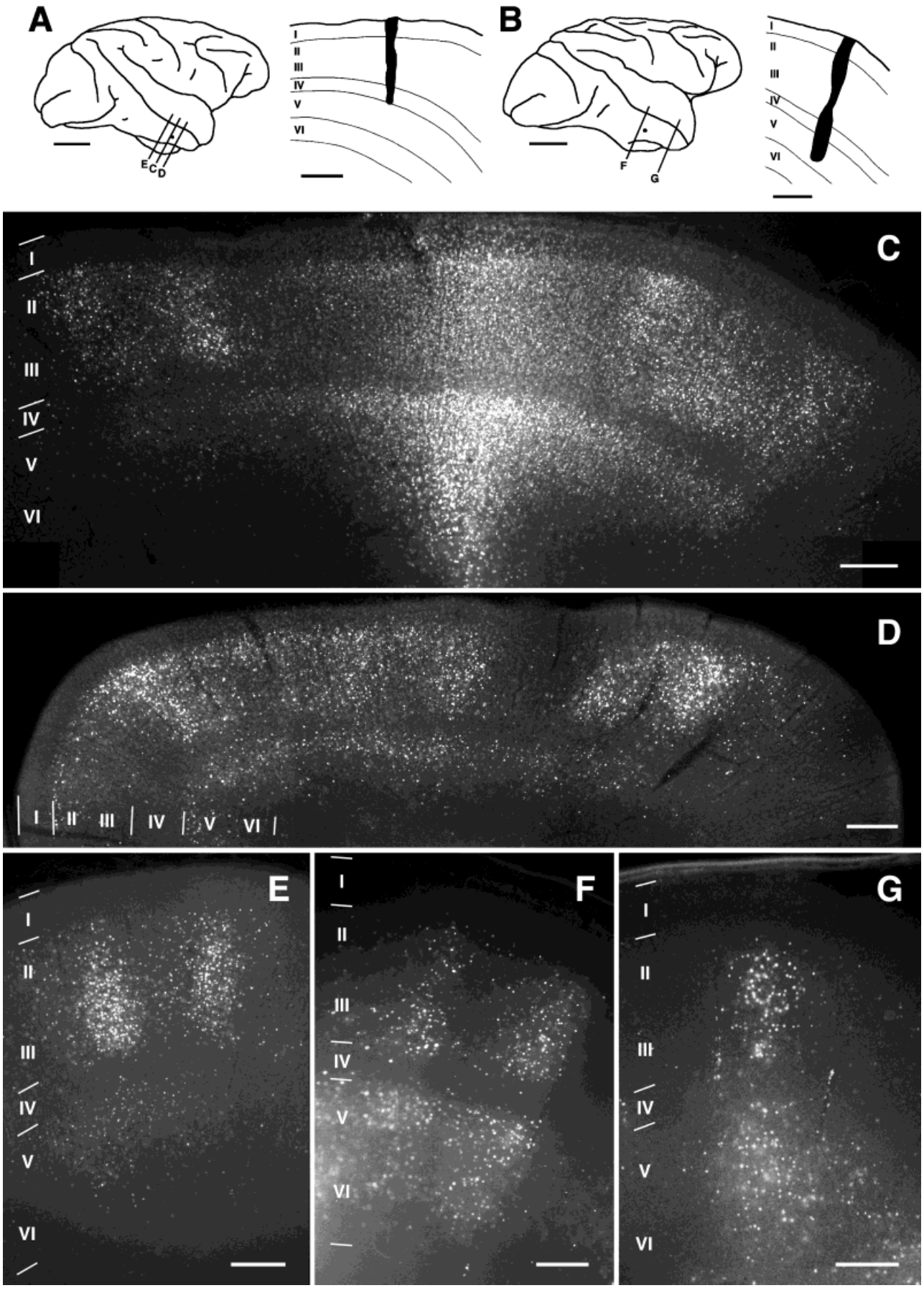

Figure 2

paraformaldehyde in 0.1 M PB, followed by 2 liters of 4% paraformaldehyde, 0.2% picric acid, 0.1% glutaraldehyde in 0.1 M PB, and 2 liters of 4% paraformaldehyde in 0.1 M PB (Kubota et al., 1993, modified for monkeys). The brains were removed, blocked, postfixed for 1–3 hours in the last fixative, and soaked in 0.1 M PB containing a graded series of sucrose (15–30%). Frozen sections were cut tangentially at 30 μm and rinsed in 0.1 M PBS. Sections were incubated in the primary antiserum, rabbit anti-GABA (Sigma) diluted 1:1,000 in 0.1 M PBS containing 4% normal goat serum (NGS), 2% bovine serum albumin (BSA, Sigma), and 0.4% Triton X-100 for 38–43 hours at 4°C. After rinsing, the sections were incubated in a secondary antiserum, either rhodamine-conjugated donkey anti-rabbit IgG (for FB-labeled sections; Chemicon, Temecula, CA) or biotinylated goat anti-rabbit IgG (for bead-labeled sections; Vector, Burlingame, CA) diluted 1:100–200 in 0.1 M PBS containing 4% NGS and 2% BSA, for 3 hours at room temperature. Bead-containing sections were then rinsed and incubated overnight at 4°C in the avidin-biotinylated horseradish peroxidase complex (Vector). After rinsing, the peroxidase reaction product was visualized by incubation in 0.1 M PBS containing 0.05% diaminobenzidine, 0.02% ammonium nickel sulfate, and 0.004% hydrogen peroxide. The incubation was performed in the dark to prevent the potential photoconversion of the fluorescent tracers. The sections were mounted onto gelatin slides, air dried, coverslipped with Vectashield (Vector), and stored in the dark at 4°C.

To evaluate the specificity of the GABA antiserum, control sections were processed using the same method described above, except that the primary antiserum was omitted. In these controls, GABA-like immunoreactivity was completely abolished.

Data analysis

The distribution of retrogradely labeled cells and GABA-immunoreactive cells was examined under a microscope (Optiphot-2, or Eclipse E-800; Nikon) equipped with fluorescent optics. Double-labeled (GABA-immunoreactive and retrogradely labeled) cells were recognized by switching between the appropriate filters for each labeling. For selected sections, retrogradely labeled cells and double-labeled cells were plotted using a computer-aided plotting system (Neurolucida, Microbrightfield, Colchester, VT). For other sections, images were digitally captured at a regular spacing under the microscope (at 4× or 10×) by using a color chilled-3CCD camera (C5810; Hamamatsu Photonics, Hamamatsu, Japan) linked to a computer. Using graphic software (Photoshop; Adobe, San Jose, CA), the contrast and brightness of images were adjusted to maximize the visibility of labeled neurons. The positions of labeled cells were calculated using the public domain NIH Image software (developed at the U.S. National Institutes of Health, Bethesda, MD). Every third or fourth section was stained for Nissl substance with cresyl violet to determine laminar boundaries.

A total of 223 LY-filled neurons were examined under a fluorescence microscope, and 95 LY-filled neurons were scanned under a confocal microscope (LSM410; Carl Zeiss, Oberkochen, Germany; 488-nm argon laser) to analyze the dendritic morphology in detail. Fifty to 100 optically sectioned images at 1-μm intervals were collected and combined to form single images of entire neurons. Slices containing LY-filled neurons were photographed using a 4× objective, under both brightfield and epifluorescent conditions, to determine the layer where the labeled neurons resided (Fig. 4). The stria of Baillarger were used as landmarks to differentiate between the layers (de Lima et al., 1990; Fujita and Fujita, 1996). Some slices containing LY-filled neurons whose laminar locations were difficult to determine under these conditions were counterstained with m-phenylenediamine (Quinn and Weber, 1988).

RESULTS

Laminar distribution of horizontally projecting neurons

Injections of the neuronal tract tracers, DY, FB, and fluorescent latex beads, retrogradely labeled TE neurons in a characteristic laminar distribution pattern. Figure 2 shows examples of sections cut perpendicular to the pia mater after DY injections into two hemispheres. Labeled neurons appeared in layers 2, 3, 5, and 6, but rarely in layers 1 and 4, except in the immediate vicinity of the injection sites where labeled neurons appeared in layers 1 and 4 as well (Fig. 2C). When a dye deposit was confined to layers 1 to 4 (Fig. 2A), labeled neurons appeared mainly in layers 2 and 3, whereas layer 5 contained a smaller number of labeled neurons and only a few neurons in layer 6 (Fig. 2C–E). When an injection deposit reached layer 5 beyond the superficial and middle layers (Fig. 2B), numerous labeled neurons appeared in layers 5 and 6 (Fig. 2F). This suggests a general segregation in trajectories between the horizontal axons in the supragranular layer and those in the infragranular layer.

At distances of more than about 1 mm from the injection site, labeled neurons were not uniformly distributed, but appeared in clusters with various degrees of distinctness (Fig. 2C–G, see also Fig. 3). Since the clusters in the supragranular layer were vertically in register with those in the infragranular layer, the densely distributed sites appeared as columns with an interruption in layer 4. Distinct columnar clusters were likely to be found at more distant sites from the injection site (Fig. 2E,F). The mean tangential width of these distinct clusters measured in layer 3 was 350 μm (SD = 110 μm; n = 21 clusters in two monkeys). Sometimes two columnar clusters appeared in tandem with a gap containing a few labeled neurons having a similar or slightly smaller width (Fig. 2E,F). Because TE does not have a band-like or stripe-like appearance in labeled tangential sections (see Fig. 3), tandem labeling of structures indicates that the clusters

Fig. 2. Laminar distribution of retrogradely labeled neurons after DY injections into TE. **A,B:** Left: The sites of the injections (dots) and the planes of the sections shown in C–G (straight lines). Right: Drawings of the sections at the center of the injection sites. The core region (dark area) in A did not enter layer V, whereas the one in B covered layers I–V. **C–G:** Photographs of sections cut perpendicular to the surface. Distances of the sections from the injection core are (C) 750 μm, (D) 1,500 μm, (E) 3,250 μm, (F) 2,250 μm, and (G) 8,150 μm. Retrograde labeling was rarely observed in layer IV except in the portion immediately adjacent to the injection site. Note that the clustered, columnar distribution of labeled neurons is particularly obvious in sections distant from the injection site (E–G). The injection covering the infragranular layer (B) yielded columnar clusters of labeled neurons extending to layer VI (F,G). Scale bars = 10 mm in A, B left, 500 μm in A,B right, 300 μm in C–G.

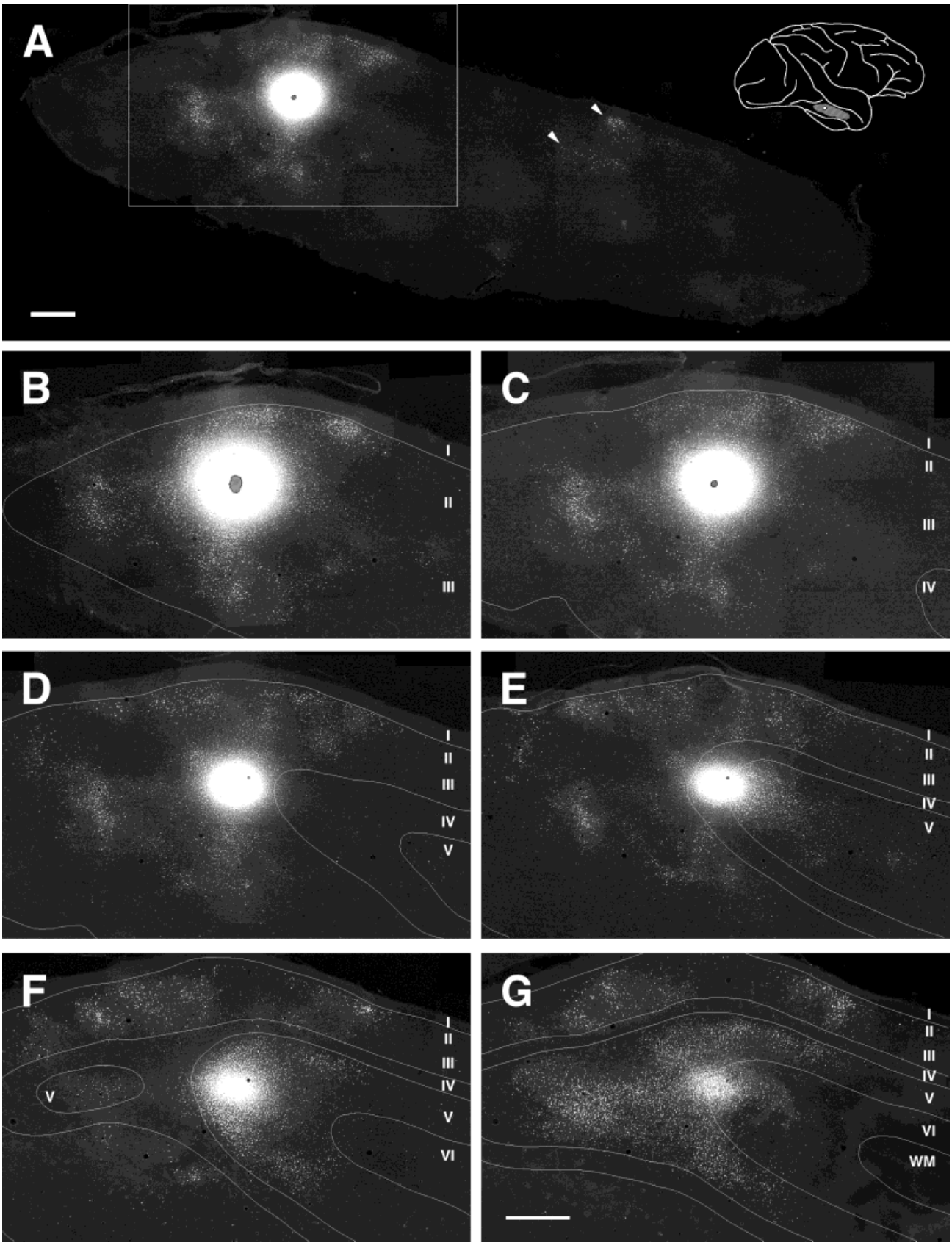
A
B
I
II
III
C
I
II
III
IV
D
I
II
III
IV
V
E
I
II
III
IV
V
F
I
II
III
IV
V
VI
V
G
I
II
III
IV
V
VI
WM

Figure 3

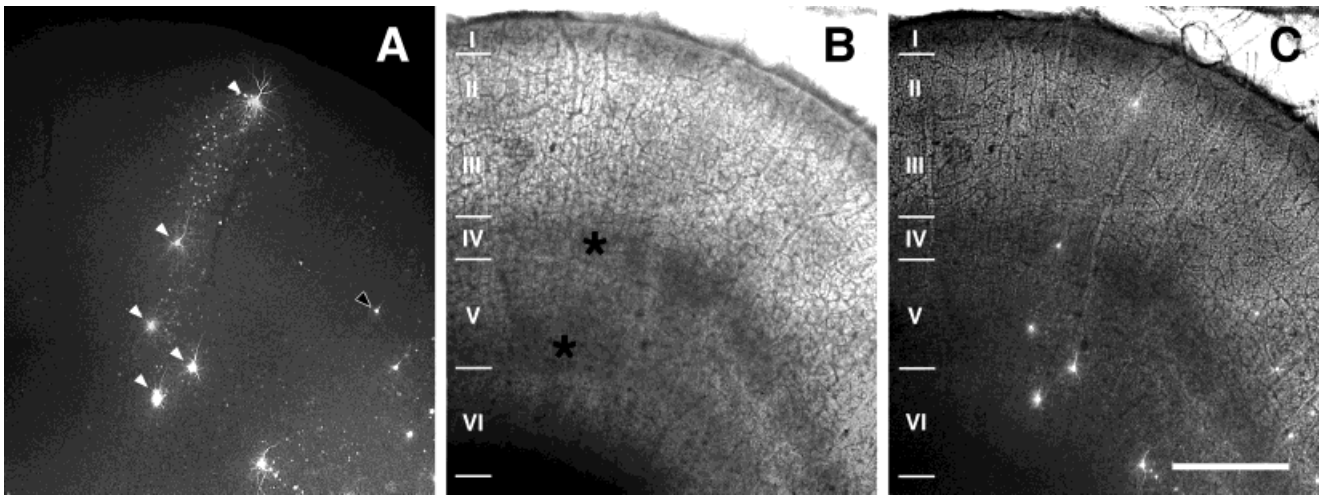

Fig. 4. Intracellular injections of Lucifer Yellow (LY) into retrogradely labeled neurons in lightly fixed slices. **A:** Fluorescence photomicrograph of a slice containing LY-filled cells. LY injections were made into both cells within the clusters of retrogradely labeled neurons (white arrowheads) and those between the clusters (black arrowhead). **B:** Brightfield photomicrograph of the slice shown in A. Asterisks indicate the external and internal stria of Baillarger. **C:** Photomicrograph taken under simultaneous fluorescence and brightfield illumination. LY-filled cells were assigned to cortical layers under this condition using the stria of Baillarger as laminar landmarks. Scale bar = 500 μm.

maintain their columnar confinement without branching into adjacent columns.

The columnar clustering of neurons appeared more distinct in layers 2 and 3 than in layers 5 and 6. Near the injection site, labeled neurons formed a continuous sheet in the infragranular layer, whereas labeling in the supragranular layer appeared more interrupted or patchy (Fig. 2C,D). At distant isolated columns, the width of the clusters was broader in the infragranular than in the supragranular layer (Fig. 2F). The columnar clusters shown in Figure 2G appeared 8 mm anterior to the injection site (see Fig. 2B for location), which likely reflects extrinsic area-to-area projections (see Discussion).

Tangential distribution of horizontally projecting neurons

In five injection cases, the tangential distribution of retrograde labeling was examined in the sections cut parallel to the pia mater. Most of the retrogradely labeled neurons were spread over distances of up to 6 mm from the center of the injection sites. Figure 3 shows examples of tangential sections of TE from a monkey that received an injection of DY into the superficial cortical layer. As we observed in cross-sections (Fig. 2), DY-labeled cells appeared uniformly up to a radius of about 1 mm around the injection site, and they were distributed in a patchy manner farther away from the injection site. Note that the labeled patches were aligned across serial tangential sections in the supragranular layer, confirming that these patches were vertically columnar in shape (Fig. 3B–E). It is also obvious in tangential sections that labeled cells in the infragranular layer were distributed more diffusely than those in the supragranular layer (Fig. 3F,G). Some of the patches of retrogradely labeled cells appeared 6.3–8.9 mm anterior to the injection sites (Fig. 3A, arrowheads) and were aligned across layers 2, 3, 5, and 6. Because they were a large distance away from the labeled cells in the vicinity of the injection site, they are interpreted as representing cells that give rise to extrinsic connections (see Discussion).

Fig. 3. Tangential distribution of retrogradely labeled neurons after a DY injection confined to the supragranular layer of TE. **A:** An entire tangential section obtained from a flattened TE. This section was cut through layers II and III. Arrowheads indicate patches of labeled neurons which appeared in the anterior part of TE and were separated from the other clusters of labeled cells surrounding the injections site. The **inset,** upper right, schematically shows the injection sites and the sectioned area on a lateral view of the brain. **B–G:** Series of sections through the area demarcated by the rectangle in A. Depths are (B) 600 μm, (C) 800 μm, (D) 1,000 μm, (E) 1,200 μm, (F) 1,400 μm, and (G) 1,600 μm from the brain surface. The speckled areas and solid lines indicate the injection core and the layer boundaries, respectively. Because labeled neurons were densely distributed in the vicinity of the injection site, they appear as single bright regions in the photographs. Note the more diffuse distribution of labeled neurons in layer V than in layers II and III (G). WM, white matter. Scale bars = 1 mm.

Intracellular labeling of horizontally projecting neurons

In lightly fixed slices, LY was injected intracellularly into 223 TE neurons which were retrogradely prelabeled with DY, and their somatic and dendritic morphology was classified as typical pyramidal, asymmetrical pyramidal, vertical fusiform, inverted pyramidal, or multipolar (de Lima et al., 1990; Good and Morrison, 1995). The laminar location of these cells was unambiguously determined by switching between brightfield and epifluorescent illumination (Fig. 4). They consisted of 131 supragranular (layers 2 and 3) neurons, four layer 4 neurons, and 88 infragranular (layers 5 and 6) neurons.

The vast majority of the injected cells (198 out of 223) were pyramidal or asymmetrical pyramidal neurons (Table 1). The labeled pyramidal neurons included a variety of

TABLE 1. Number and Distribution of Morphological Types of Lucifer Yellow–Filled Neurons in TE

	Morphological types					
Layer	Pyramidal	Asymmetrical pyramidal	Vertical fusiform	Inverted pyramidal	Multipolar	Total
I	0	0	0	0	0	0
II/III	130	0	0	0	1	131
IV	4	0	0	0	0	4
V	34	6	4	2	1	47
VI	12	12	16	1	0	41
Total	180	18	20	3	2	223

subtypes and sizes (Fig. 5), but they did not include the large pyramidal cells in layer 5 which have a thick apical dendrite ascending up to layer 1 and are known to project to subcortical structures. In the supragranular layer, 130 of the 131 injected neurons had a morphology typical of pyramidal neurons, i.e., cell bodies with a pyramidal or somewhat spherical shape, well-differentiated apical and basal dendrites, symmetrical spreading of the basal dendrites, and many spines on the dendrites (Fig. 5A–E). In the infragranular layer, 46 of the 88 injected neurons (52%) were symmetrical pyramidal cells (Fig. 5F,G), and 18 (20%) were asymmetrical pyramidal cells with one of their basal dendrites well developed compared to the other basal dendrites (Fig. 5H,I). The other 24 neurons (27%) in the infragranular layer did not exhibit pyramidal cell–like morphology. Twenty of them were classified as vertical fusiform neurons whose cell body was elongated in the radial direction with two thick dendrites, one directed toward the pial surface and the other directed toward the white matter (Fig. 6A,D; de Lima et al., 1990). Some of these fusiform neurons possessed numerous dendritic spines (Fig. 6B,C), and others possessed relatively few spines (Fig. 6D). In addition, there were three inverted pyramidal neurons (Fig. 6E,G) with spines on their dendrites (Fig. 6F,H).

Among the 223 LY-filled neurons, only two neurons were identified unequivocally as interneurons. One neuron (Fig. 6I) was found in layer 2 and was 530 μm from the center of the injection site. The cell body was oval and 13 μm across its major diameter. Five thin and curving dendrites with smooth surfaces emanated from the soma, and most of their branches ascended toward the pia mater. This cell was similar to the layer II extraverted multipolar neurons described in the cat primary auditory cortex (Prieto et al., 1994). The other neuron (Fig. 6J) was found in layer 5 and was 400 μm from the center of the injection site. The cell body was oval and 19 μm across its major diameter. Dendrites emanated from the soma in all directions, but most of those projecting toward layer 6 were truncated at the slice surface.

To examine whether any morphological differences existed between the short- and long-range projection neurons, LY-filled neurons were classified according to their distance from the injection site (Table 2). Typical, asymmetrical, and inverted pyramidal cells appeared evenly both near (<2 mm) and far (>2 mm) from the injection site, whereas fusiform cells were more frequently labeled at distant sites (>2 mm) than at near sites (χ^2 test, $P < .05$). We also compared the morphological type of LY-filled neurons that were inside or outside of the clusters. For this analysis, we examined only LY-filled neurons unambiguously determined to be inside or outside of the clusters, excluding neurons near the boundary of the clusters. No significant difference in the cell type between the two regions was found (Table 3).

Double labeling with retrograde tracer and GABA immunocytochemistry

As only a few horizontally projecting neurons were classified as interneurons, we performed GABA immunocytochemistry on retrogradely labeled sections to further characterize the identity, proportion, and distribution of horizontally projecting interneurons. We used two tracers, FB and fluorescent latex beads, for retrograde labeling in this analysis. FB was a sensitive retrograde tracer which labeled remote cells, but it caused necrosis of tissue ~500 μm around the injection core, making it difficult to identify GABA-immunoreactive cells in this region. In contrast, injection of beads resulted in a smaller number of weakly labeled neurons in the remote regions, but analysis of the area near the injection sites was possible because of their non-toxic and less-diffusable nature. DY was not used in this experiment because, during the incubation of slices in the antiserum solution, DY drastically diffused from the labeled neurons to surrounding cells to yield false double-positive cells.

In the first experiment, we performed GABA immunocytochemistry on the sections which were previously injected with FB. Out of the 2,547 FB-labeled cells counted in 11 sections across all layers, only nine cells (0.4%) were immunoreactive for GABA (Fig. 7A,B, Table 4). Within a radius of 1 mm from the injection site center, seven FB-labeled cells (2.3%) were GABA-immunoreactive, whereas at distances greater than 1 mm from the injection site center, only two FB-labeled cells (0.1%) were GABA-immunoreactive. The farthest double-labeled neuron was 3.2 mm from the injection site center and was found in layer 5.

In the second experiment using fluorescent latex beads as the retrograde tracer, retrogradely labeled neurons were unambiguously identified even within 500 μm from the injection core (Fig. 8). Out of the 2,062 beads-containing cells in four sections, two from the supragranular layer and the other two from the infragranular layer, 114 cells (5.5%) were GABA-immunoreactive, and 90 of these were located within a radius of 500 μm from the injection site center (Table 4). In the annulus between 500 and 1,000 μm around the injection site, 23 (4.3%) of 537 beads-containing cells were GABA-immunoreactive (5.0% in the supragranular layer; 2.6% in the infragranular layer). Double-labeled neurons were found scattered in every direction around the injection site. In the region beyond a radius of 1 mm from the injection site center, only one (0.4%) of 231 beads-containing cells exhibited GABA immunoreactivity.

Thus, the vast majority of double-labeled cells appeared within 1 mm of the injection where retrogradely labeled cells did not form clear clusters. Outside this range, only three neurons were double labeled. We therefore could not determine whether the fraction of GABA-immunoreactive "inside-cluster-cells" and "outside-cluster-cells" are the same.

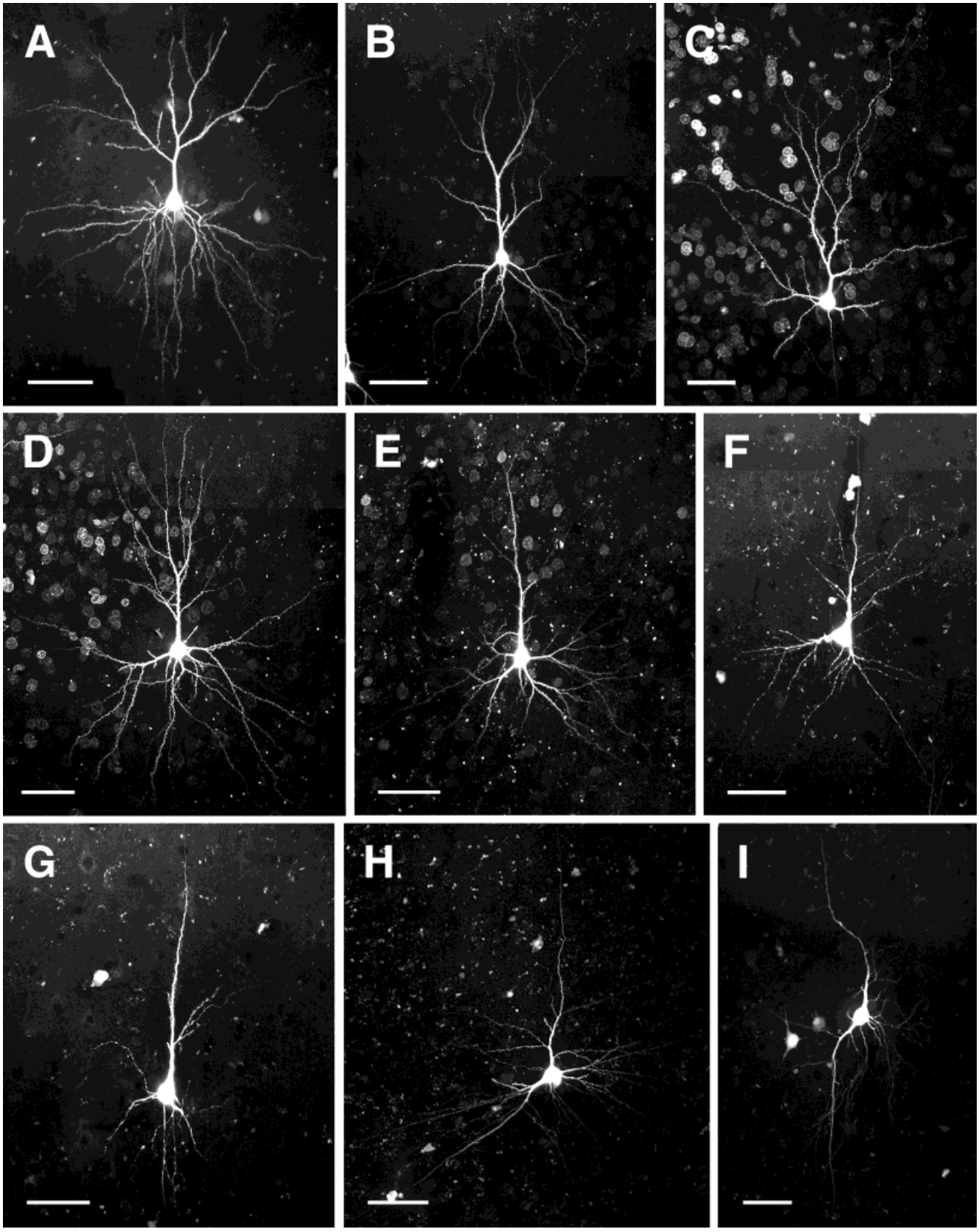

Fig. 5. Confocal microscopic images of retrogradely labeled, LY-filled pyramidal neurons. **A–G:** Projection neurons with typical pyramidal morphology in layers II (A–C), III (D,E), V (F), and VI (G). **H,I:** Asymmetric pyramidal neurons in layers V (H) and VI (I). Images taken near the injection sites contain other retrogradely labeled neurons in the backgrounds (C–E). The pial surface is toward the top of each photograph. Scale bars = 50 μm.

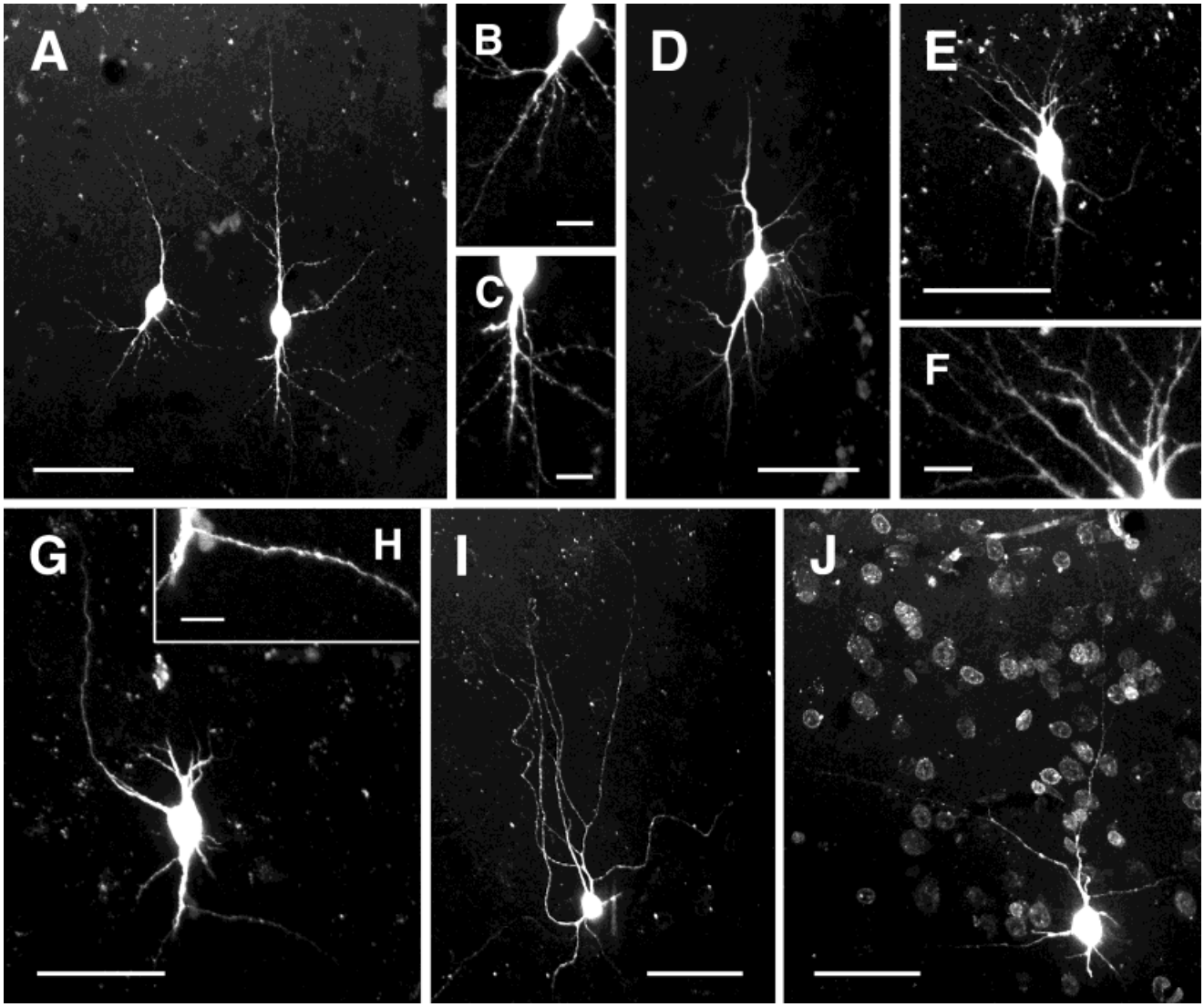

Fig. 6. Confocal microscopic images of retrogradely labeled, LY-filled nonpyramidal neurons. **A–D:** Vertical fusiform neurons in layers V (A) and VI (D). High-magnification images of spinous dendrites of the neurons in A are shown in B and C. **E–H:** Inverted-pyramidal neurons in layers V (E) and VI (G). High-magnification images of spinous dendrites of the neurons in E and G are shown in F and H, respectively. **I,J:** Multipolar interneurons in layers II (I) and V (J) with spine-free dendrites. These two neurons were located at lateral distances of 530 μm (I) and 400 μm (J) from the injections site center. The pial surface is toward the top of each photograph. Scale bars = 50 μm in A,D,E,G,I,J, 10 μm in B,C,F,H.

TABLE 2. Distance From the Injection Site Center of Different Types of Lucifer Yellow–Filled Neurons in TE

Layer	Distance from the injection site center	Morphological types					Total
		Pyramidal	Asymmetrical pyramidal	Vertical fusiform	Inverted pyramidal	Multipolar	
II/III	<2 mm	49	0	0	0	1	50
	>2 mm	81	0	0	0	0	81
V/VI	<2 mm	16	2	1	2	1	22
	>2 mm	30	16	19	1	0	66
Total		176	18	20	3	2	219

DISCUSSION

The present retrograde tracing study in the macaque monkey has demonstrated that 1) horizontally projecting retrogradely labeled TE neurons were predominantly located in layers 2, 3, 5, and 6; 2) they were uniformly distributed immediately around the injection site and tended to appear in columnar clusters at a distance from the injection, particularly in layers 2 and 3; 3) the majority of them were spiny neurons of various types, such as

TABLE 3. Spatial Distribution of Different Types of Lucifer Yellow–Filled Neurons With Respect to Clusters in TE[1]

Layer	Site of neurons	Morphological types					Total
		Pyramidal	Asymmetrical pyramidal	Vertical fusiform	Inverted pyramidal	Multipolar	
II/III	Inside clusters	48	0	0	0	0	48
	Outside clusters	51	0	0	0	0	51
V/VI	Inside clusters	26	6	10	0	0	42
	Outside clusters	12	9	9	2	0	32
Total		137	15	19	2	0	173

[1]We did not count the neurons that were located on the borders of clusters or near the injection sites.

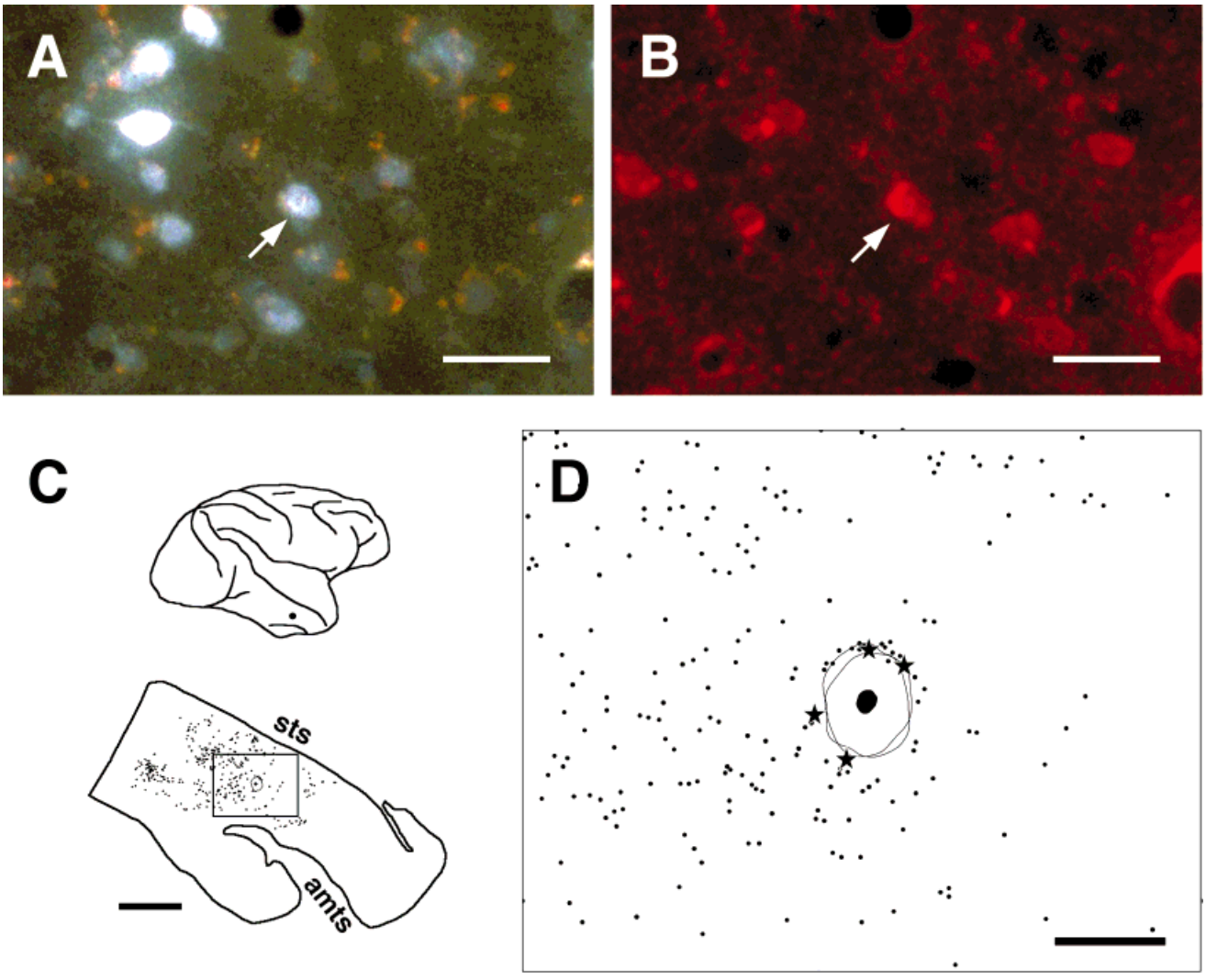

Fig. 7. γ-Aminobutyric acid (GABA) -immunoreactive horizontally projecting neurons in TE. **A:** Fluorescence photomicrograph of Fast Blue (FB)-labeled neurons in layer III, 0.8 mm from the center of the injection site. **B:** Brightfield photomicrograph of the same field of view as in A. A double-labeled cell (arrow) contains both FB and GABA immunoreactivity. **C:** The site of the FB injection (dot) is shown in the top drawing. The distribution of FB-labeled cells (dots) on a section cut tangentially through the infragranular layer is shown in the bottom drawing. **D:** The area demarcated by the rectangle in C is plotted in detail. Reconstruction was made from two sections separated by 150 μm through the infragranular layer. The dark area represents the injection core, and the solid lines around the core demarcate the diffusion zone of FB (zone 1 of Condé, 1987). Small dots and stars mark the positions of FB-labeled cells and double-labeled cells, respectively. Tracer-free GABA-immunoreactive cells were distributed throughout the entire section (not shown), whereas most of the double-labeled cells were found in the immediate vicinity of the diffusion zone. Scale bars = 30 μm in A, and B, 5 mm in C (bottom), 500 μm in D.

symmetrical and asymmetrical pyramidal cells and vertical fusiform cells, all of which were assumed to be excitatory neurons; and 4) GABAergic interneurons contributed little to the long-range (>1 mm) horizontal connections. Each of these findings is discussed in relation to previous studies in TE and other cortical areas, with a consider-

TABLE 4. Proportion of Neurons Double-Labeled by Retrograde Tracer and GABA Immunocytochemistry in TE

Monkey	Retrograde tracer	Layers	Proportion of GABA-immunoreactive neurons <500 μm[1]	500–1,000 μm	>1,000 μm
A08L	Fast Blue	II–VI	4.0%[2] (4/100)[3]	1.4% (3/208)	0.1% (2/2239)
A10R	Beads	II/III	8.4% (70/833)	5.0% (19/381)	0.6% (1/156)
A10R	Beads	V/VI	4.3% (20/461)	2.6% (4/156)	0.0% (0/75)
Total			6.7% (94/1394)	3.5% (26/745)	0.1% (3/2470)

[1]Distance form the injection site center.
[2]Percentages indicate the proportion of retrogradely labeled neurons which expressed GABA immunoreactivity.
[3]Number of double-labeled neurons/number of retrogradely labeled neurons.

ation of the physiological implications of these results on information processing in TE.

Laminar distribution of cells of origin of horizontal axons

Retrogradely labeled cells appeared in layers 2, 3, 5, and 6, but only a few layer 4 cells were labeled beyond a radius of 1 mm from the injection site center. This is consistent with our previous report that injections of biocytin confined to layer 4 of TE do not label cells and axons beyond 1 mm lateral to the injection site (Fig. 8 in Fujita and Fujita, 1996). The restricted lateral projections of layer 4 cells compared to cells in other layers are a common feature reported for various cortices in monkeys. Tracer injections confined to layer 4 result in limited lateral labeling (e.g., area V4, Yoshioka et al., 1992; areas 9 and 46 in the prefrontal cortex, Levitt et al., 1993). Columnar clusters of retrogradely labeled cells with few labeled cells in layer 4 have also been found after injections to different animals and areas; for example, area 17 of rat (McDonald and Burkhalter, 1993) and ferret (Ruthazer and Stryker, 1996), and area V2 (Rockland, 1985) and areas 9 and 46 in the prefrontal cortex (Kritzer and Goldman-Rakic, 1995) of monkey. However, in the primate V1 where layer 4 is differentiated into four sublaminae, neurons in layer 4B project laterally up to 2–3 mm and form patches of axons, whereas neurons in the other sublaminae (4A, 4Ca, 4Cb) do not exhibit this feature (Rockland and Lund, 1983). An even more marked exception has been reported for cat area 18, where columnar clusters of retrogradely labeled neurons contain the largest number of labeled cells in layer 4 (Matsubara et al., 1987). Although in that study wheat germ agglutinin–conjugated horseradish peroxidase (WGA-HRP) was used as a retrograde tracer, this does not explain the difference between our results and theirs. In our hands WGA-HRP also failed to label layer 4 cells in the columnar clusters in TE (I. Fujita, unpublished observation).

Our findings revealed clusters of labeled cells in the supragranular layer in line with those in the infragranular layer so as to give a columnar appearance. This clustering was denser in layers 2 and 3 than in layers 5 and 6, however. Neurons within the inferior temporal cortex (TE as well as the cortex in the ventral bank of the superior temporal sulcus) that project to the ipsilateral prefrontal cortex also cluster in patches in layers 3 but are distributed rather continuously in layers 5 and 6 (de Lima et al., 1990). As in other cortices, axons descending from layer 3 neurons in TE give off laterally spreading collateral arborizations in layer 5 (Fujita and Fujita, 1996). These distinctions suggest that horizontal interactions within the infragranular layer are more diffusely organized compared to those in the supragranular layer where interconnections occur in a more restricted cluster-to-cluster manner.

Tangential distribution of cells of origin of horizontal axons

Most of the patchy clusters of labeled neurons appeared within 6 mm of the injection site. This tangential spread is greater than that reported for V1, which is typically 1.5–2.0 mm in the supragranular layer (Rockland and Lund, 1983; Livingstone and Hubel, 1984), but is consistent with the anterograde labeling results in TE (Fujita and Fujita, 1996). In fact, two or three clusters of labeled neurons sometimes appeared beyond this extent, 8 mm anterior to the injection given in the posterior part of TE (Fig. 3A, arrowheads). Such remote patches of anterogradely labeled axons have been found in the anterior part of TE after injections of biotinylated dextran amine in the posterior TE (H. Tanigawa and I. Fujita, unpublished observation). Because some of these remote axonal patches were formed by axons passing through the white matter, they are considered to reflect extrinsic (i.e., area-to-area) connections between the anterior and posterior parts of TE. Although it is difficult to establish in our present materials whether the remote clusters of retrogradely labeled neurons reflect intrinsic or extrinsic connections, we interpret that these remote clusters represent extrinsic projections from a yet-to-be-defined subdivision in the anterior part of TE to the posterior TE, given that their distribution was so far removed from the other clusters surrounding the injection site.

Soma-dendritic morphology of cells of origin of horizontal axons

The vast majority of horizontally projecting neurons were typical or modified pyramidal neurons. Our sample contained relatively fewer cells within a radius of 0.5 mm from the center of DY injection sites. This was because the strong fluorescence surrounding the injection site disturbed our ability to accurately impale cells in this region with a glass micropipette. Nevertheless, except for this, the data obtained from LY-filled cells are not likely to suffer from a technical bias. For instance, although we observed an infrequent number of LY-filled nonpyramidal cells, this was not due to a sampling bias based on an inability to impale them. In fact, we determined from random injections of unlabeled neurons that about 30% of the sampled cells were nonpyramidal cells, such as double bouquet cells or bipolar cells (data not shown). This proportion of nonpyramidal cells corresponds to the previously reported proportion (24%) of GABA-immunoreactive neurons in TE (Hendry et al., 1987). Moreover, the DY tracer did not interfere with the ability to assess the morphology of a LY-filled cell because DY labels only the nucleus. And the sample of LY-filled cells we analyzed most likely incorporated multiple cell types because we injected neurons in all layers, within clusters and between clusters, at the center and at the edge of clusters, and strongly and faintly DY-labeled neurons (see Fig. 4).

Studies by de Lima et al. (1990) characterized the dendritic morphology of TE neurons that were retrogradely labeled by tracer injections into the ipsilateral

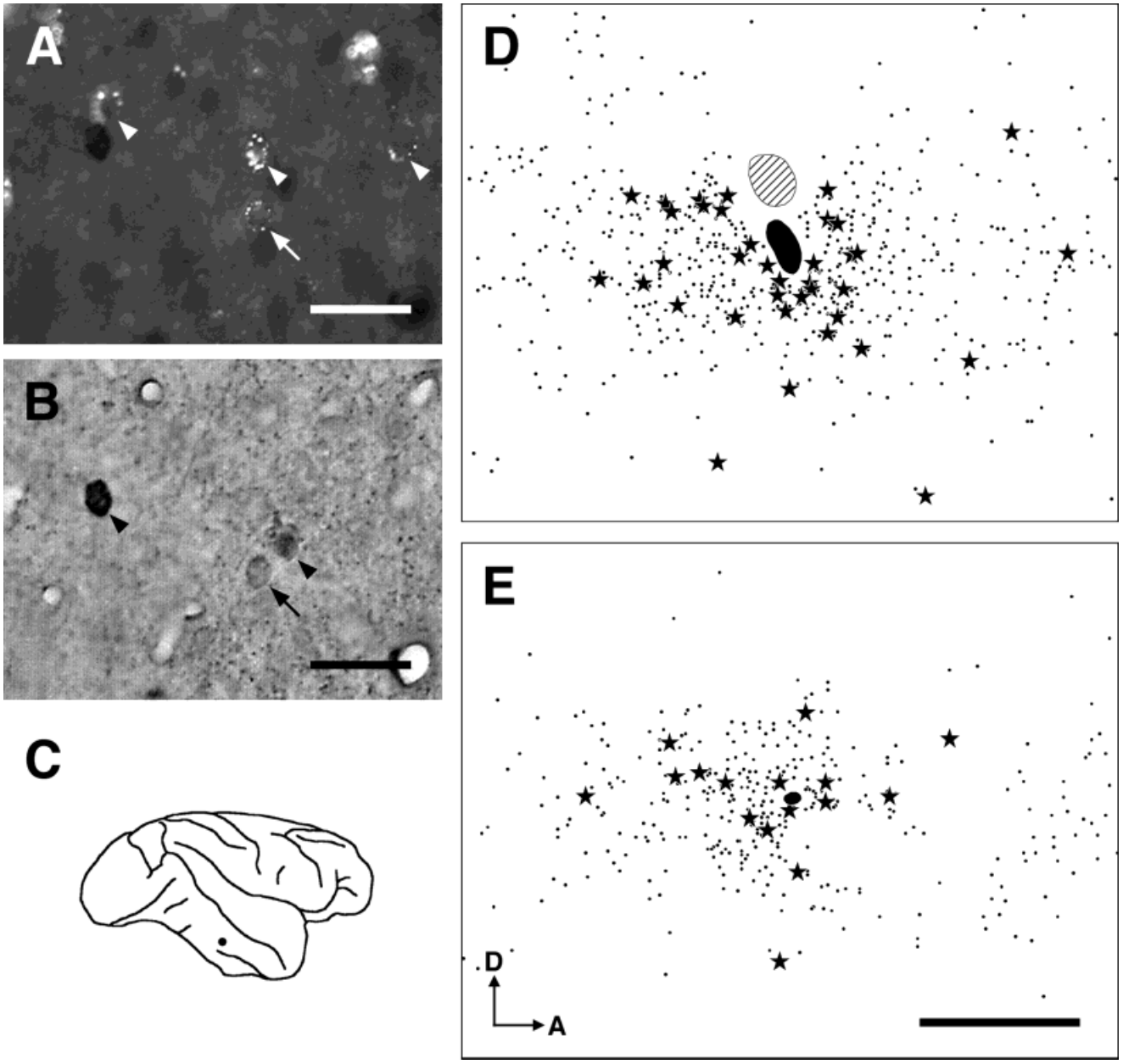

Fig. 8. Photomicrographs and distribution of the latex microsphere (bead) -containing and GABA-immunoreactive neurons in TE. **A:** Fluorescent photomicrograph of bead-containing neurons in layer III, 0.6 mm from the center of the injection site. **B:** Brightfield photomicrograph of the same microscopic field as in A. A double-labeled cell (arrow) contains both beads and GABA immunoreactivity. Cells indicated by arrowheads in A contain beads but not GABA immunoreactivity. In B, arrowheads point to single-labeled GABA-immunoreactive neurons. **C:** The site of the beads injection (dot). **D,E:** Plots of beads-containing (small dots) and double-labeled cells (stars) in tangential sections through the superficial layer (D) and the infragranular layer (E). The dark areas represent the injection core, and the hatched area indicates the injections site of a different tracer for another experiment. A, anterior; D, dorsal. Scale bars = 30 μm in A, B, 500 μm in E (also applies to D).

prefrontal cortex. They found that 1) dendrites from a given cell do not extend to all layers, but are confined to just a few layers, and 2) neurons projecting to the ipsilateral prefrontal cortex consist of a heterogeneous population of spiny cells (typical and asymmetrical pyramidal cells and vertical and horizontal fusiform cells). This description resembles that of the cells that give rise to the intrinsic horizontal axons in TE, except that we found retrogradely labeled inverted pyramidal cells but no horizontal fusiform cells. Caution should be taken, however, when characterizing dendritic morphology from intracellular injections in lightly fixed slices. In these preparations, the somata of the impaled cells must lie within 50 μm of the cut surface of the slices. Otherwise, the scattering of light causes the cell to be blurred, diminishing its ability to be injected with precision. Therefore, in these slices, it is

likely that the distal parts of some dendrites of the impaled cells were truncated at the cut surfaces.

In our samples of LY-filled neurons, most of the vertical fusiform cells were located at a distance more than 2 mm from the injections site. An interpretation might be that vertical fusiform neurons participate in long-range (>2 mm) horizontal interactions, but not in short-range (<2 mm) interactions. However, a more parsimonious explanation relies on the fact that vertical fusiform cells are most often found in those sites where the cortex is curved (i.e., the shoulder of sulci; Tömböl, 1984). Because our tracer injections were aimed at the crown of the inferior temporal gyrus where the curvature is minimal and few vertical fusiform cells reside, this could explain why we observed more of these cells at a distance (>2 mm) from the injection site.

The morphology of horizontally projecting neurons has also been studied in layer 2/3 of cat area 18 (Thejomayen and Matsubara, 1993), where most of the retrogradely labeled, LY-filled neurons were spiny pyramidal neurons of various subtypes. Smooth multipolar projection neurons were also seen primarily within 1 mm of the injection site, as in the present study.

GABA immunoreactivity of horizontally projecting neurons

In the supragranular layers, our results of double-staining TE neurons using retrograde tracers and a GABA immunocytochemistry agree well with those experiments previously performed in area 17 (Albus et al., 1991) and area 18 (Matsubara and Boyd, 1992) of cat and in the primary visual cortex of rat (McDonald and Burkhalter, 1993): 1) The proportion of double-labeled neurons is small (5%, Albus et al., 1991; 3–11%, Matsubara and Boyd, 1992), and 2) most of them appear near the injection site (within a radius of 1 mm). In rat primary visual cortex (McDonald and Burkhalter, 1993) and cat area 18 (Matsubara and Boyd, 1992), double-labeled neurons are more widely distributed in the infragranular layer than in the supragranular layer. But in TE, there was no significant difference in the spread of double-labeled neurons between the infragranular and supragranular layers (Table 4).

It has been shown in areas 17 and 18 in cats that large basket cells in layer 3 have axons extending laterally up to 1.8 mm from the somata (Somogyi et al., 1983; Kisvárday and Eysel, 1993; Kisvárday et al., 1993). These cells possess characteristic smooth varicose dendrites and can be easily identified. Our sample of intracellularly labeled neurons did not include a typical cell of this type, although such GABA-immunoreactive retrogradely labeled large basket cells may reside particularly at a distance from the injection site.

In summary, across diverse cortices, including the primary sensory cortices to higher association cortices such as TE, most of the cells from which intrinsic horizontal axons originate are either pyramidal or other spiny cells, suggesting that they are excitatory neurons. Several morphological differences exist, however, between the horizontal axonal patches in TE and those in V1. These differences are likely to reflect those of pyramidal and other spiny neurons. Inhibitory interneurons both in TE and V1, by contrast, project horizontally only a short distance, usually less than 1 mm, suggesting that the nature of the inhibitory interneuron circuitry does not underlie the formation of a patchy or a continuous brain map.

Organization of the horizontal axon system in TE

The spatial distribution of cells that give rise to horizontal axons which converge at a given site provide us with insights into the interactions between columns in TE. The presence of retrogradely labeled neurons uniformly distributed in the immediate vicinity of the injection site identified in the present study, along with injection halo of anterogradely labeled axons carrying numerous boutons described in previous studies (Amir et al., 1993; Fujita and Fujita, 1996), suggests that a given site or column in TE interacts with surrounding neighbors via horizontal axons as well as recurrent collaterals. This is consistent with the recent results obtained by Wang, Y. et al. (1996) who microiontophoretically applied a GABA antagonist, bicuculline methiodide (BMI), into the immediate vicinity of TE neurons. In the presence of BMI, some TE cells began to respond to visual stimuli that did not normally evoke responses. This effect was observed only for a particular range of stimuli which often activated other neurons along the same or surrounding recording tracks. This suggests that TE neurons may receive subthreshold excitatory inputs from nearby sites which are masked by local GABA-mediated inhibition under normal conditions.

In contrast to the apparently uniform connections between nearby sites, the connections between distant sites are not diffuse or uniform, but are organized in a specific column-to-column manner. The cells with long-range projections to columnar patches are mostly pyramidal and spiny fusiform neurons, suggesting that their synaptic action is probably excitatory. Given that multiple columns with similar stimulus selectivities were observed in previous physiological experiments (Fujita et al., 1992; Wang, G. et al., 1996), it is very likely that such distant sites connected by horizontal axons share, at least in part, stimulus selectivity for object features. This will be clarified in future physiological experiments combined with neuronal tracing techniques.

ACKNOWLEDGMENTS

We thank Lawrence C. Katz, Yoshiyuki Kubota, and Toshio Terashima for technical advice, Xu Lihua and Wang Quanxin for help in surgery and immunocytochemistry, and Emiko Sugitani and Tomoko Maeda for secretarial assistance. One of the animals used was obtained through the Cooperation Research Program of Primate Research Institute, Kyoto University.

This work was supported by grants to I.F. from CREST of the Japan Science and Technology Corporation, The Uehara Memorial Foundation, and the Ministry of Education, Science, Sports and Culture.

LITERATURE CITED

Albus, K., P. Wahle, J. Lübke, and C. Matute (1991) The contribution of GABA-ergic neurons to horizontal intrinsic connections in upper layers of the cat's striate cortex. Exp. Brain Res. *85:*235–239.

Amir, Y., M. Harel, and R. Malach (1993) Cortical hierarchy reflected in the organization of intrinsic connections in macaque monkey visual cortex. J. Comp. Neurol. *334:*19–46.

Condé, F. (1987) Further studies on the use of the fluorescent tracers fast blue and diamidino yellow: Effective uptake area and cellular storage sites. J. Neurosci. Methods *21:*31–43.

Dean, P. (1976) Effects of inferotemporal lesions on the behavior of monkeys. Psychol. Bull. *83:*41–71.

de Lima, A.D., T. Voigt, and J.H. Morrison (1990) Morphology of the cells within the inferior temporal gyrus that project to the prefrontal cortex in the macaque monkey. J. Comp. Neurol. *296:*159–172.

Felleman, D.J. and D.C. Van Essen (1991) Distributed hierarchical processing in the primate cerebral cortex. Cereb. Cortex *1:*1–47.

Fujita, I. (1993) Columns in the inferotemporal cortex: Machinery for visual representation of objects. Biomed. Res. *14 (Suppl. 4):*21–27.

Fujita, I. (1997) The inferior temporal cortex: columns and horizontal axons. In H. Sakata, A. Mikami, and J.M. Fuster (eds): The Association Cortex: Structure and Function. Amsterdam: Harwood Academic Publishers, pp. 259–268.

Fujita, I. and T. Fujita (1996) Intrinsic Connections in the macaque inferior temporal cortex. J. Comp. Neurol. *368:*467–486.

Fujita, I., K. Tanaka, M. Ito, and K. Cheng (1992) Columns for visual features of objects in monkey inferotemporal cortex. Nature *360:*343–346.

Fujita, I., H. Tanigawa, H. Ojima, and M. Kato (1995) Neurons mediating horizontal interactions in the monkey inferior temporal cortex. Soc. Neurosci. Abstr. *21:*660.

Good, P.F. and J.H. Morrison (1995) Morphology and kainate-receptor immunoreactivity of identified neurons within the entorhinal cortex projecting to superior temporal sulcus in the cynomolgus monkey. J. Comp. Neurol. *357:*25–35.

Gross, C.G. (1973) Visual functions of inferotemporal cortex. In R. Jung (ed): Handbook of Sensory Physiology. Berlin: Springer-Verlag, pp. 451–482.

Hendry, S.H.C., H.D. Schwark, E.G. Jones, and J. Yan (1987) Numbers and proportions of GABA-immunoreactive neurons in different areas of monkey cerebral cortex. J. Neurosci. *7:*1503–1519.

Hubel, D.H. and T.N. Wiesel (1977) Functional architecture of macaque monkey visual cortex. Proc. R. Soc. Lond. [Biol.] *198:*1–59.

Katz, L.C. and D.M. Iarovici (1990) Green fluorescent latex microspheres: A new retrograde tracer. Neuroscience *34:*511–520.

Kisvárday, Z.F. and U.T. Eysel (1993) Functional and structural topography of horizontal inhibitory connections in cat visual cortex. Eur. J. Neurosci. *5:*1558–1572.

Kisvárday, Z.F., C. Beaulieu, and U.T. Eysel (1993) Network of GABAergic large basket cells in cat visual cortex (area 18): Implication for lateral disinhibition. J. Comp. Neurol. *327:*398–415.

Kritzer, M.F. and P.S. Goldman-Rakic (1995) Intrinsic circuit organization of the major layers and sublayers of the dorsolateral prefrontal cortex in the rhesus monkey. J. Comp. Neurol. *359:*131–143.

Kubota, Y., S. Mikawa, and Y. Kawaguchi (1993) Neostriatal GABAergic interneurones contain NOS, calretinin or parvalbumin. Neuroreport *5:*205–208.

Levitt, J.B., D.A. Lewis, T. Yoshioka, and J.S. Lund (1993) Topography of pyramidal neuron intrinsic connections in macaque monkey prefrontal cortex (areas 9 and 46). J. Comp. Neurol. *338:*360–376.

Livingstone, M.S. and D.H. Hubel (1984) Specificity of intrinsic connections in primate primary visual cortex. J. Neurosci. *4:*2830–2835.

Logothetis, N.K. and D.L. Sheinberg (1996) Visual object recognition. Annu. Rev. Neurosci. *19:*577–621.

Matsubara, J.A. and J.D. Boyd (1992) Presence of GABA-immunoreactive neurons within intracortical patches in area 18 of the cat. Brain Res. *583:*161–170.

Matsubara, J.A., M.S. Cynader, and N.V. Swindale (1987) Anatomical properties and physiological correlates of the intrinsic connections in cat area 18. J. Neurosci. *7:*1428–1446.

McDonald, C.T. and A. Burkhalter (1993) Organization of long-range inhibitory connections within rat visual cortex. J. Neurosci. *13:*768–781.

Mishkin, M., L.G. Ungerleider, and K.A. Macko (1983) Object vision and spatial vision: Two cortical pathways. Trends Neurosci. *6:*414–417.

Nelson, M.E. and J.M. Bower (1990) Brain maps and parallel computers. Trends Neurosci. *13:*403–408.

Ojima, H. (1993) Dendritic arborization patterns of cortical interneurons labeled with the lectin, Vicia villosa, and injected intracellularly with Lucifer yellow in aldehyde-fixed rat slices. J. Chem. Neuroanat. *6:*311–321.

Prieto, J.J., B.A. Peterson, and J.A. Winer (1994) Morphology and spatial distribution of GABAergic neurons in cat primary auditory cortex (AI). J. Comp. Neurol. *344:*349–382.

Quinn, B. and E. Weber (1988) m-phenylenediamine: a novel fluorescent Nissl like stain for neuroanatomy. Soc. Neurosci. Abstr. *14:*547.

Rockland, K.S. (1985) A reticular pattern of intrinsic connections in primate area V2 (area 18). J. Comp. Neurol. *235:* 467–478.

Rockland, K.S. and J.S. Lund (1983) Intrinsic laminar lattice connections in primate visual cortex. J. Comp. Neurol. *216:*303–318.

Ruthazer, E.S. and M.P. Stryker (1996) The role of activity in the development of long-range horizontal connections in area 17 of the ferret. J. Neurosci. *16:*7253–7269.

Somogyi, P., Z.F. Kisvárday, K.A.C. Martin, and D. Whitteridge (1983) Synaptic connections of morphologically identified and physiologically characterized large basket cells in the striate cortex of cat. Neuroscience *10:*261–294.

Suzuki, W. (1996) Neuroanatomy of the monkey entorhinal, perirhinal and parahippocampal cortices: Organization of cortical inputs and interconnections with amygdala and striatum. Semin. Neurosci. *8:*3–12.

Tanaka, K. (1996) Inferotemporal cortex and object vision. Annu. Rev. Neurosci. *19:*109–139.

Tanigawa, H. and I. Fujita (1997) Topographical relation between horizontal projections from adjacent sites in the macaque inferior temporal cortex: A double anterograde labeling study. Soc. Neurosci. Abstr. *23:*2062.

Thejomayen, D.M. and J.A. Matsubara (1993) Confocal microscopic study of the dendritic organization of patchy, intrinsic neurons in area 18 of the cat. Cereb. Cortex *3:*442–453.

Tömböl, T. (1984) Layer VI cells. In A. Peters and E.G. Jones (eds.): Cerebral Cortex, Vol. 1, Cellular Components of the Cerebral Cortex. New York: Plenum Press, pp. 479–519.

von Bonin, G. and P. Bailey (1947) The Neocortex of *Macaca mulatta*. Urbana: The University of Illinois Press.

Wang, G., K. Tanaka, and M. Tanifuji (1996) Optical imaging of functional organization in the monkey inferotemporal cortex. Science *272:*1665–1668.

Wang, Y., I. Fujita, and Y. Murayama (1996) Role of GABAergic inhibition in generation of visual response properties of inferior temporal cortex neurons in the monkey. Soc. Neurosci. Abstr. *22:*1614.

Xu, L.H., H. Tanigawa, and I. Fujita (1997) Distribution of AMPA-type glutamate receptors along the ventral visual cortical pathway in the macaque: A gradient reflecting the cortical hierarchy. Soc. Neurosci. Abstr. *23:*2062.

Yoshioka, T., J.B. Levitt, and J.S. Lund (1992) Intrinsic lattice connections of macaque monkey visual cortical area V4. J. Neurosci. *12:*2785–2802.